

# Projectile Fragmentation of relativistic nuclei in peripheral Collisions

Swarnapratim Bhattacharyya<sup>1</sup>, Maria Haiduc<sup>2</sup>, Alina Tania Neagu<sup>2</sup> and Elena Firu<sup>2</sup>

<sup>1</sup>Department of Physics, New Alipore College, L Block, New Alipore, Kolkata 700053, India

Email: swarna\_pratim@yahoo.com

<sup>2</sup>Institute of Space Science, Bucharest, Romania

**PACS No. 25.75.-q**  
**25.75.Ag.**

## Abstract

A study of multiplicity distribution of singly charged, doubly charged, multi charged projectile fragments and shower particles have been carried out for the peripheral collisions in <sup>16</sup>O-emulsion, <sup>22</sup>Ne-emulsion and <sup>28</sup>Si-emulsion interactions at an incident momentum of (4.1-4.5) AGeV/c. Events having no target fragments have been designated as peripheral collision events. Percentage of peripheral events has been found to increase with the increase of projectile mass. Dispersion of the multiplicity distribution and its dependence on projectile mass for projectile fragments and shower particles has also been investigated. Dependence of average multiplicity of projectile fragments and shower particles on the mass of the projectile beam has been studied. Study of different fragmentation mode during the emission of multi charged projectile fragments has also been carried out.

## Introduction

Heavy ion collisions provide us a unique opportunity to study the extended state of matter under extremes of density and temperature reachable otherwise in the hot early universe. At high densities and temperatures, a phase transition of hadronic matter to quark–gluon plasma (QGP) is expected. The subsequent investigation of the QGP state is the main objective of studying the relativistic heavy ion experiments [1, 2]. Many scientists, both experimentalists and theoreticians are searching for the possible signals of QGP. Thus, the studies of high-energy nucleus–nucleus collisions are the most important research topic in particle and nuclear physics. Apart from searching the QGP signal in multiparticle production, studies of nuclear fragmentation is also important in high energy interactions. In comparison to the study of multiparticle production, the study of nuclear fragmentation received rather limited attention. The world of nuclear fragmentation should also be explored in order to have detail knowledge of high energy collisions. Nuclear fragmentation has been considered to be one of the most important aspects of heavy-ion collisions, since it has been speculated that the decay of a highly excited nuclear system might carry information about the equation of state and the liquid–gas phase transition of low-density nuclear matter. In nuclear fragmentation, both the target and the projectile can go into disintegration yielding target and projectile fragments respectively [3]. The fragmentation of relativistic projectile nucleus is of great significance as it leads to the emission of fragments with a broad mass spectrum which extends from the lightest fragments, the nucleons to the fragments as heavy as the disintegrating projectiles. This allows us to extract information on the fragmentation mechanism involved in such processes. The study of projectile fragmentation reflects some important features of heavy ion collisions and has encouraged the scientists to perform experiments with projectile fragmentation [4-17]. Depending on the collision geometry, nucleus-nucleus collisions can be divided into three categories namely central collisions, quasi-central collisions and peripheral collisions. In the central collisions, the projectile and target overlap, number of projectile spectator is zero and no projectile fragments are emitted. Central collisions create favourable environment to study the QGP phase transition. As the centrality of the collision is decreased projectile spectators begin to increase in number. Peripheral collisions are visualised to occur when the impact parameter is nearly equal to the sum of the radii of the target and the projectile nuclei.

Despite their hidden art of physics, peripheral collisions have attracted a limited interest. In fact their study has been overshadowed by the study of central and near central collisions. Peripheral collision is the best situation of studying the projectile fragmentation. The projectile and the target nuclei in peripheral collisions are far apart, so a small momentum is transferred between the interacting nuclei. A detailed study of the projectile fragment makes it possible to go on to the search for complicated quasi-stationary states of fragments. In the nuclear scale of distances and excitations they can possess properties which make them analogous to dilute quantum gases in atomic physics at ultra-cold temperatures. The existence of such systems can find some important applications for the problems of nuclear astrophysics. In this respect, the fragment jets are a microscopic model of stellar media.

Goal of this study is the exploration of projectile fragmentation in the peripheral nucleus-nucleus collisions using nuclear emulsion track detector. There is no doubt that the experiments performed in RHIC and LHC in recent times have many advantages in the study of relativistic particle production, which is related to the formation of quark-gluon plasma (QGP). However, for the study of projectile fragmentation, the accelerator experiment with the fixed target has more advantages. Nuclear emulsion detectors offer a good angular resolution ( $\sim 0.1\text{mrad}$ ) and high spatial resolution which makes it possible to detect all the projectile fragments of charge  $Z \geq 1$  in the  $4\pi$  geometry. Nuclear emulsion track detector is well suited to study the different fragmentation mode during multi-fragment emission process.

## Experimental Details

In order to get the required data for the present analysis NIKFI-BR2 emulsion pellicles of dimension  $20\text{cm} \times 10\text{ cm} \times 600\ \mu\text{m}$  were irradiated by the  $^{16}\text{O}$  (at an incident momentum of 4.5 AGeV/c),  $^{22}\text{Ne}$  (at an incident momentum of 4.1 AGeV/c) and  $^{28}\text{Si}$  beam (at an incident momentum of 4.5 AGeV/c) accelerated from the Synchrophasotron at Joint Institute of Nuclear Research (JINR), Dubna, Russia [18].

The emulsion pellicles were exposed horizontally to the incoming projectile beams. When a projectile collides with the target present in nuclear emulsion an interaction or an event occurs. In order to find an interaction or an event we have scanned the emulsion plate along the track of the incident beam starting from the entry point of the beam into the emulsion plate until an interaction occurs. We have also performed the scanning slowly in the backward direction from the interaction point along the track of the incident beam to ensure that the interaction selected by forward scanning did not include interaction from the secondary tracks of other interactions so that we can select only the primary interactions and exclude the secondary ones. Scanning in the forward and backward directions by two different observers increases the efficiency of selecting a primary event and its vertex up to 99%. More details about scanning and measurement can be found from our earlier publication [18]. After scanning those events were selected where the incident beam lie within  $3^\circ$  from the direction of the main beam in the pellicle [18]. This criterion ascertains that the real projectile beam has been selected for the analysis. Events showing interactions close to the emulsion surface and glass surface (interactions within  $20\ \mu\text{m}$  from the top and bottom surface of the pellicle) were excluded from our consideration. Rejection of such events reduces the losses of tracks and minimizes the uncertainties in the measurements of emission and azimuthal angles [18]. According to the criteria mentioned above, we have chosen 2823 inelastic interactions for the  $^{16}\text{O}$  projectile, 4308 inelastic interactions of the  $^{22}\text{Ne}$  projectile and 1310 inelastic interactions of the  $^{28}\text{Si}$  projectile.

According to the Powell, in nuclear emulsion track detector, particles emitted and produced from an interaction can be classified into four categories, namely the projectile fragments, shower particles, the grey particles and the black particles [19]. Details characteristics of these particles have been given below.

**Projectile Fragments:** The projectile fragments are the spectator parts of the incident projectile nucleus that do not directly participate in an interaction. They are emitted within a very narrow extremely forward cone, called the Fermi cone. The Fermi cone is characterized by a semi-vertex angle  $\theta_f$  where  $\theta_f = P_{Fermi} / P_{inc}$ . Here  $P_{inc}$  is the incident projectile momentum per nucleon measured in GeV/c and  $P_{Fermi}$  is the Fermi momentum in GeV/c of the nucleons of the projectile fragments. The value of  $P_{Fermi}$  can be calculated based on Fermi gas model of the nucleus and the numerical value of  $P_{Fermi}$  comes out to be 0.21 GeV/c. Having almost the same energy or momentum per nucleon as the incident projectile, these fragments exhibit uniform ionization over a long range and suffer negligible scattering. The main sources of the projectile fragments are nucleons and nucleon clusters formed in the nuclear collisions. Projectile fragments can be further classified according to their charges as singly charged ( $Z=1$ ), doubly charged ( $Z=2$ ) and multi-charged ( $Z > 2$ ) projectile fragments.

(i) Singly charged projectile fragments have ionisation  $I$  less or equal to  $1.4I_0$ .  $I_0$  is the minimum ionization of a singly charged particle. Multiplicity of singly charged fragments is denoted by  $N_p$ .

(ii) Doubly charged projectile fragments are denoted by  $N_\alpha$ . They have ionisation  $I \cong 4I_0$  and no change in their ionization can be noticed when the tracks are followed up to a distance of approximately 2 cm from the vertex of interaction.

(iii) Multi-charged projectile fragments are denoted by  $N_F$ . They have ionisation  $I > 6I_0$  and no change in their ionization can be noted when their tracks are followed up to a distance of approximately 1 cm from the vertex of interaction. Charge of these fragments can be measured by the delta ray counting method.

**Shower particles:** The tracks of particles having ionization  $I$  less or equal to  $1.4I_0$  are called shower tracks. The shower particles are mostly pions (about more than 90%) with a small admixture of kaons and hyperons (less than 10%). These shower particles are produced in a forward cone. The velocities of these particles are greater than  $0.7c$  where  $c$  is the velocity of light in free space. Because of such a high velocity, these particles are not generally confined within the emulsion pellicle. Energies of these shower particles lie in the GeV range. Average multiplicity of shower particles can be denoted by  $\langle N_s \rangle$ .

**Grey particles:** Grey particles are mainly fast target recoil protons with energies up to 400 MeV. They have ionization  $1.4 I_0 \leq I < 10 I_0$ . Ranges of these particles are greater than 3 mm in the emulsion medium. These grey particles have the velocities lying between  $0.3c$  and  $0.7c$ . Average multiplicity of grey particles is denoted by  $\langle N_g \rangle$ .

**Black particles:** Black particles consist of both singly and multiply charged fragments. They are fragments of various elements like carbon, lithium, beryllium etc with ionization greater or equal to  $10I_0$ . These black particles have the maximum ionizing power. They are less energetic and consequently they are short ranged. In the emulsion medium, ranges of black particles are less than 3 mm. The velocities of the black particles are less than  $0.3c$ . In emulsion experiments, it is very difficult to measure the charges of the target fragments. Therefore, it is not possible to identify the exact nucleus. Average multiplicity of black particles is denoted by  $\langle N_b \rangle$ . Total number of black and grey tracks in an event is known as heavy tracks and is denoted by  $N_h$ .

In this paper we present the experimental results on the multiplicity distribution of singly charged, doubly charged and multi charged projectile fragments and also of shower particles in peripheral collisions for  $^{16}\text{O}$ -emulsion,  $^{22}\text{Ne}$ -emulsion and  $^{28}\text{Si}$ -emulsion interactions at an incident momentum of (4.1-4.5) AGeV/c. The study of different fragmentation mode of multi charged fragment emission has also been performed.

## Results and Analysis

In order to study the multiplicity distribution of singly charged ( $Z=1$ ), doubly charged ( $Z=2$ ), multi charged ( $Z>2$ ) projectile fragments and the shower particles in peripheral collisions we have selected the events without any target excitation causing the total number of black and grey tracks to be zero ( $N_b + N_g = N_h = 0$ ) as the peripheral events from 2823 inelastic interactions for the  $^{16}\text{O}$  projectile, 4308 inelastic interactions of the  $^{22}\text{Ne}$  projectile and 1310 inelastic interactions of the  $^{28}\text{Si}$  projectile in nuclear emulsion detector. The number of events along with the percentage of events (POE) having  $N_h=0$  have been tabulated in table 1. From the table it may be noticed that percentage of events (POE) in peripheral collisions increases with the increase of mass number  $A_p$  of the projectile beam. Figure 1 shows the variation of percentage of peripheral events (POE) with the mass of the projectile beam for  $^{16}\text{O}$ -emulsion,  $^{22}\text{Ne}$ -emulsion and  $^{28}\text{Si}$ -emulsion interactions at an incident momentum of

(4.1-4.5) AGeV/c. Errors shown in the figure are statistical errors only. We have tried to fit the variation of percentage of events (POE) without target fragmentation ( $N_h = 0$ ) with the mass number of the projectile beam  $A_p$  with a function of the form  $POE = aA_p^b$ . The values of the fitting parameters  $a$  and  $b$  have been calculated on the basis of the  $\chi^2$  minimization method. Calculated values of  $a$  and  $b$  have been found to be  $a = 6.74 \pm .06$  and  $b = .198 \pm .003$  with  $\chi^2$  per degrees of freedom values .98.

The average multiplicity of singly charged ( $N_p$ ) doubly charged ( $N_\alpha$ ) and multi charged projectile fragments ( $N_F$ ) along with the produced shower particles in the peripheral events have been presented in table 2 for the three interactions. From the table it may be noted that within the experimental error average multiplicity of singly charged ( $N_p$ ) and doubly charged ( $N_\alpha$ ) fragments show an increasing trend with the increase of projectile mass. Moreover from the table it may be noted that for each projectile the values of average multiplicity of projectile fragments for  $Z=1$  are higher than those for  $Z=2$  and  $Z>2$ .

From the table it may also be noted that in case of shower particles the average multiplicity increases smoothly with the increase of projectile mass. We have studied the variation of the average multiplicity of shower particles with the mass number of the projectile beam  $A_p$ . The variation of average shower particle multiplicity with mass number of the projectile beam has been presented in figure 2. Errors shown in figure 2 are of statistical origin. The errors of average multiplicity have been calculated on the basis of a subjective estimate calculated from the sample standard deviation. The variation has been parametrized by a relation  $\langle N_s \rangle = aA_p^b$ . The values of the fitting parameters have been evaluated on the basis of the  $\chi^2$  minimization method. We have also calculated the values of the non-linear regression coefficient ( $R^2$ ) for the fits in order to quantify the goodness of the fit. The values of the fitting parameters,  $\chi^2$  per degrees of freedom ( $\chi^2 / DOF$ ) value of the fit and the values of non-linear regression coefficient ( $R^2$ ) of the fit are given in table 3. The exponent  $b$  characterises the increment of average shower particle multiplicity with the mass of the projectile beam. In a very recent paper [20] we have shown that in central collisions of  $^{16}\text{O-AgBr}$ ,  $^{22}\text{Ne-AgBr}$  and  $^{28}\text{Si-AgBr}$  interactions at an incident momentum of (4.1-4.5) AGeV/c, the increment of  $\langle N_s \rangle$  with  $A_p$  can be parametrized as  $\langle N_s \rangle = (3.34 \pm .11)A_p^{(.75 \pm .08)}$ . While in this paper we see that for peripheral collisions average shower

particle multiplicity increases with  $A_P$  as  $\langle N_S \rangle = (1.23 \pm .09)A_P^{(.24 \pm .07)}$ . Thus for peripheral collisions increment of  $\langle N_S \rangle$  with  $A_P$  is rather slow in comparison to central collisions.

Average multiplicity of multi-charged projectile fragments ( $Z > 2$ ) are found to increase with the increase of projectile mass as evident from table 2. We have investigated the variation of the average multiplicity of multi-charged projectile fragments with the mass number of the projectile beam  $A_p$ . The variation of average multiplicity of multi-charged projectile fragments with mass number of the projectile beam has been shown in figure 3. Errors associated with the experimental points are the statistical errors only. The variation has been parametrized by a relation  $\langle N_F \rangle = aA_p^b$ . The method of the  $\chi^2$  minimization has been applied in this case also to extract the values of the fitting parameters  $a$  and  $b$ . We have also calculated the values of the non-linear regression coefficient ( $R^2$ ) for the fits in order to quantify the goodness of the fit. The values of the fitting parameters,  $\chi^2$  per degrees of freedom ( $\chi^2 / \text{DOF}$ ) value of the fit and the values of non-linear regression coefficient ( $R^2$ ) of the fit are given in table 3. From table 3 it may be said that average multiplicity of multi-charged fragments varies with the projectile mass  $A_p$  according to the relation  $\langle N_F \rangle = (.065 \pm .005)A_p^{(.76 \pm .07)}$ .

Multiplicity distribution of projectile fragments having charge  $Z=1$  and  $Z=2$  along with the multiplicity distribution of shower particles for the peripheral events have been presented in fig 4(a)-4(c) for  $^{16}\text{O}$ -emulsion interactions, in fig 5(a)-5(c) for  $^{22}\text{Ne}$ -emulsion interactions and in fig 6(a)-6(c) for  $^{28}\text{Si}$ -emulsion interactions. From the multiplicity distribution of the projectile fragments it may also be pointed out that the probability of producing singly charged and doubly charged projectile fragments decreases as the number of these fragments increases. In table 4 we have presented the values of the maximum number of projectile fragments (for both  $Z=1$  and  $Z=2$ ) emitted in a single event for each of the projectiles. Table 4 reflects that maximum number of singly charged ( $Z=1$ ) and doubly charged ( $Z=2$ ) projectile fragments emitted in single event is highest for Si projectile.

From the figures it may be noted that the height of the multiplicity distribution of singly charged fragments decreases with the increase of projectile mass. However for doubly charged fragments no such observation can be made as evident from the table where peak of the distribution occurs for  $^{22}\text{Ne}$ -emulsion interactions. Interestingly from the multiplicity

distribution of shower particles no systematic dependence of height and width of the distribution on the mass number of the projectile beam can be found. The multiplicity distributions of multi-charged fragments for the three interactions have been shown in fig7. From the figure it is clear that height of the multiplicity distribution for multi-charged fragments increases with the increase of projectile mass.

In order to study the multiplicity distribution of the singly charged, doubly charged, multi charged projectile fragments and the shower particles in peripheral events of the three interactions in more details we have calculated the dispersion of the multiplicity distribution following the relation  $D = \sqrt{\langle N^2 \rangle - \langle N \rangle^2}$ . The width of the multiplicity distribution is characterised by the parameter D. The calculated values of the dispersion D have been presented in table 5 for singly charged , doubly charged , multi charged projectile fragments and shower particles in peripheral events in case of  $^{16}\text{O}$ -emulsion,  $^{22}\text{Ne}$ -emulsion and  $^{28}\text{Si}$ -emulsion interactions at an incident momentum of (4.1-4.5) AGeV/c. From the table it may be seen that with the increase of projectile mass the values of the dispersion increases for the singly charged, doubly charged projectile fragments and for the shower particles. However for multi charged fragments dispersion D decreases with the increase of projectile mass.

In order to understand the dynamics of projectile fragmentation we have also studied the fragmentation mode of multi-fragment emission in the peripheral events of  $^{16}\text{O}$ -emulsion,  $^{22}\text{Ne}$ -emulsion and  $^{28}\text{Si}$ -emulsion interactions at an incident momentum of (4.1-4.5) AGeV/c. In table 6 we have presented the values of the probability of producing one projectile fragments of charge  $Z > 2$  and two projectile fragments of charge  $Z > 2$  along with the probability of producing projectile fragments of charge  $Z > 2$  with and without the emission of any  $\alpha$  particles. From the table it may be said that probability of producing one projectile fragments of charge  $Z > 2$ , two projectile fragments of charge  $Z > 2$  and the probability of producing projectile fragments of charge  $Z > 2$  with the emission of  $\alpha$  particles increases with the increase of projectile mass. While the probability of emitting projectile fragments of charge  $Z > 2$  without the emission of any  $\alpha$  particles do not show any systematic variation with the mass number of the projectile beam. Moreover it is evident from the table that the probability of emitting more than one fragment of charge  $Z > 2$  is significantly smaller than that of emitting one projectile fragment of charge  $Z > 2$ . This view has also been supported in

[21]. From table 6 it may be noticed that for  $^{22}\text{Ne}$ -emulsion and  $^{28}\text{Si}$ -emulsion interactions the emission of projectile fragments of charge  $Z>2$  accompanied by the emission of  $\alpha$  particles is more probable than that of without the emission of  $\alpha$  particles. On the contrary for  $^{16}\text{O}$ -emulsion interactions the probability of emission of projectile fragments of charges  $Z>2$  without the emission of  $\alpha$  particles is higher in comparison to the emission of  $Z>2$  charged fragments accompanied by the emission of  $\alpha$  particles.

### Conclusions and Outlook

To summarize we recall that we have presented a study of multiplicity distribution of singly charged, doubly charged and multi charged projectile fragments and also of shower particles in peripheral events of  $^{16}\text{O}$ -emulsion,  $^{22}\text{Ne}$ -emulsion and  $^{28}\text{Si}$ -emulsion interactions at an incident momentum of (4.1-4.5) AGeV/c. Events with complete absence of target fragmentation have been selected as peripheral events. Study of different fragmentation mode of multi-charged projectile fragments emission has also been presented. The presentation makes it possible to extract qualitative information about fragmentation of relativistic nuclei in peripheral interactions. The emulsion technique allows one to observe these systems to the smallest details and gives the possibility of studying them experimentally.

The significant conclusions of this analysis are as follows.

1. Percentage of peripheral events (POE) selected according to the criteria  $N_h = 0$  increases with the increase of projectile mass  $A_p$  according to the relation  $\text{POE} = (6.74 \pm .06)A_p^{(.198 \pm .003)}$ .
2. Average multiplicities of projectile fragments of charge  $Z=1$  and  $Z=2$  show an approximate tendency to increase with the increase of projectile mass within the experimental errors.
3. Average multiplicity of shower particle increases smoothly with the mass number of the projectile beam  $A_p$  according to the relation  $\langle N_s \rangle = (1.23 \pm .09)A_p^{(.24 \pm .07)}$ . On the other hand average multiplicity of multi-charged projectile fragments increases with  $A_p$  according to the relation  $\langle N_F \rangle = (.065 \pm .005)A_p^{(.76 \pm .07)}$ .
4. Average multiplicities of singly charged fragments are higher than those of doubly charged and multi-charged fragments.

5. Probability of producing singly charged, doubly charged and multi-charged projectile fragments decreases as the number of these fragments increases.
6. Maximum number of singly charged and doubly charged projectile fragments emitted in a single event is highest for the heaviest projectile among the three projectiles.
7. Height of the multiplicity distribution for the singly charged fragments decreases while the width of the multiplicity distribution increases with the increase of projectile mass.
8. Height of the multiplicity distribution of multi-charged fragments increases with the increase of projectile mass.
9. The dispersion of multiplicity distribution for singly charged, doubly charged projectile fragments and also for the shower particles increase with the increase of projectile mass.
10. Dispersion values of the multiplicity distribution for the multi-charged fragments decreases with the increase of projectile mass.
11. Production of single projectile fragments with charge  $Z>2$  is the most probable mode of multi-charge projectile fragments emission. This probability increases with the increase of projectile mass.
12. Probability of emission of two projectile fragments of charge  $Z>2$  is significantly small. This probability increases with the increase of projectile mass.
13. Emission of projectile fragments of charge  $Z>2$  accompanied by the emission of  $\alpha$  particle is more probable than that of without the emission of  $\alpha$  particle for  $^{22}\text{Ne}$ -emulsion and  $^{28}\text{Si}$ -emulsion interactions.
14. Probability of emission of projectile fragments of charge  $Z>2$  accompanied by the emission of  $\alpha$  particle increases with the increase of projectile mass.
15. Probability of emission of projectile fragments of charge  $Z>2$  without the emission of  $\alpha$  particle is independent of the mass of the projectile beam.

It is true that there are many papers available in the literature where a detailed study of projectile fragmentation has been carried out. However, investigations of projectile fragmentation in peripheral collisions are scanty. Essence of this paper lies in the fact that

our study of projectile fragmentation has been carried out in peripheral collisions selected by the absence of target excitation. In this respect the study is important and interesting. The observed results of this study of multiplicity distribution of projectile fragments and shower particles in peripheral events of nucleus-nucleus collisions can be viewed as an experimental fact.

### **Acknowledgement**

The authors are grateful to Prof. Pavel Zarubin, JINR, Dubna, Russia for providing them the required emulsion data. Dr. Bhattacharyya also acknowledges Prof. Dipak Ghosh, Department of Physics, Jadavpur University and Prof. Argha Deb Department of Physics, Jadavpur University, for their inspiration in the preparation of this manuscript.

### **References**

- [1] D Teaney, J Lauret and E V Shuryak Phys. Rev. Lett. 86 (2001)4783
- [2] Quark Matter 99 1999 Proc. 14th Int. Conf. on Ultra-Relativistic Nucleus–Nucleus Collisions (Torino, Italy, 10–15 May)
- [3] S. Bhattacharyya Int. Jour. of Mod. Phys E 19(2010)319
- [4] Wang Er-Qin, Chin. Phys. Lett. 28 (2011)082501
- [5]. M. I. Adamovich et al (EMU01 Collaboration), Phys. Lett. B 390 (1997) 445.
- [6]. G. Singh et al., Phys. Rev. C 43 (1991) 2417.
- [7] M. I. Adamovich et al (EMU01 Collaboration), Phys. Lett. B 338 (1994) 397.
- [8]. S. Fakhraddin and M. A. Rahim, Phys. Scripta 78 (2008) 015101.
- [9]. A. Stolz et al., Phys. Rev. C 65 (2002) 064603.
- [10]. F. H. Liu, Chin J. Phys. 39 (2001) 248.

- [11]. M. A. Jilany, Nucl. Phys. A 705 (2002) 477.
- [12]. A. Dabrowska, Acta. Phys. Pol. B 33 (2002) 1961.
- [13]. M. Nadi et al., J. Phys. G 25 (1999) 1169.
- [14]. M. Nadi et al., J. Phys. G 28 (2002) 1251.
- [15]. A. El-Naghy, M. Mohery and K. H. Gad, Acta. Phys. Hung. 15 (2002) 155.
- [16]. Ying et al., Int. J. Mod. Phys. E 17 (2008) 1319.
- [17] Magda A. Rahim and S. Fakhraddin Nucl. Phys. A 831(2009)39
- [18] S. Bhattacharyya, M.Haiduc, A.T. Neagu and E. Firu Jour. of Phys G 40(2013)025105
- [19] C.F. Powell, P.H. Fowler and D.H. Perkins “The study of elementary particles by photographic method” (Oxford, Pergamon,1959) page 450-464 and references therein
- [20] S. Bhattacharyya, M.Haiduc, A.T. Neagu and E. Firu Can. Jour of Phys. 94(2016)884
- [21] M.El-Nadi et al Jour. of Phy G 28(2002)241

**Table 1**

Interactions	Total inelastic interactions	Interactions without target fragmentation ( $N_h = 0$ )	Percentage of Interactions without target fragmentation ( $N_h = 0$ )
$^{16}\text{O}$ -emulsion (4.5 AGeV/c)	2823	330	11.68%
$^{22}\text{Ne}$ -emulsion (4.1 AGeV/c)	4308	537	12.46%
$^{28}\text{Si}$ -emulsion (4.5 AGeV/c)	1310	171	13.05%

Table 1 represents the total inelastic interactions, interactions without target fragmentation ( $N_h = 0$ ) and Percentage of Interactions without target fragmentation ( $N_h = 0$ ) for  $^{16}\text{O}$ -emulsion,  $^{22}\text{Ne}$ -emulsion and  $^{28}\text{Si}$ -emulsion interactions at an incident momentum of (4.1-4.5) AGeV/c.

**Table 2**

Interactions	Average Multiplicity of singly charged fragments $\langle N_p \rangle$	Average Multiplicity of Doubly charged fragments $\langle N_\alpha \rangle$	Average Multiplicity of Multi-Charged charged fragments $\langle N_F \rangle$	Average multiplicity of shower particles $\langle N_s \rangle$
$^{16}\text{O}$ -emulsion (4.5 AGeV/c)	$1.57 \pm .03$	$1.22 \pm .02$	$.52 \pm .05$	$2.49 \pm .11$
$^{22}\text{Ne}$ -emulsion (4.1 AGeV/c)	$1.49 \pm .14$	$1.09 \pm .21$	$.76 \pm .06$	$2.60 \pm .15$
$^{28}\text{Si}$ -emulsion (4.5 AGeV/c)	$2.49 \pm .15$	$1.44 \pm .31$	$.82 \pm .09$	$2.86 \pm .19$

Table 2 represents the values of average Multiplicity of singly charged fragments  $\langle N_p \rangle$ , average Multiplicity of Doubly charged fragments  $\langle N_\alpha \rangle$ , average Multiplicity of Multi-Charged charged fragments  $\langle N_F \rangle$  and average multiplicity of shower particles  $\langle N_s \rangle$  for  $^{16}\text{O}$ -emulsion,  $^{22}\text{Ne}$ -emulsion and  $^{28}\text{Si}$ -emulsion interactions at an incident momentum of (4.1-4.5) AGeV/c for the peripheral events (events without target fragmentation,  $N_h = 0$ ).

**Table 3**

Particles	$a$	$b$	$\chi^2 / DOF$	$R^2$
Shower particles	$1.23 \pm .09$	$.24 \pm .07$	.97	.99
Multi-Charged Fragments( $Z>2$ )	$.065 \pm .005$	$.76 \pm .07$	.94	.94

Table 3 represents the values of the fitting parameters of the plot of average multiplicity with the mass number of the projectile  $\langle N_s \rangle = aA_p^b$  in case of the shower particle multiplicity and values of the fitting parameters of the plot of average multiplicity with the mass number of the projectile beam for the multi-charged fragments  $\langle N_F \rangle = aA_p^b$ , the  $\chi^2$  per degrees of freedom ( $\chi^2 / DOF$ ) value of both the fit and the non-linear regression coefficient  $R^2$  for both the fits in case of  $^{16}\text{O}$ -emulsion,  $^{22}\text{Ne}$ -emulsion and  $^{28}\text{Si}$ -emulsion interactions at an incident momentum of (4.1-4.5) AGeV/c for the peripheral events (events without target fragmentation,  $N_h = 0$ ) in our analysis.

**Table 4**

Interactions	Z=1 (maximum value in a event)	Z=2 (maximum value in a event)
<sup>16</sup> O-emulsion (4.5 AGeV/c)	6	4
<sup>22</sup> Ne-emulsion (4.1AGeV/c)	8	5
<sup>28</sup> Si-emulsion (4.5 AGeV/c)	9	6

Table 4 represents the values of the maximum number of projectile fragments of both Z=1 and Z=2 emitted in a single peripheral event (event without target fragmentation,  $N_h=0$ ) for <sup>16</sup>O-emulsion, <sup>22</sup>Ne-emulsion and <sup>28</sup>Si-emulsion interactions at an incident momentum of (4.1-4.5)AGeV/c.

**Table 5**

Interactions	Dispersion Values $D = \sqrt{\langle n^2 \rangle - \langle n \rangle^2}$			
	Singly Charged Projectile Fragments	doubly Charged Projectile Fragments	Multi-Charged Projectile Fragments	Shower Particles
$^{16}\text{O}$ -emulsion	$1.34 \pm .02$	$1.13 \pm .01$	$.499 \pm .010$	$2.20 \pm .08$
$^{22}\text{Ne}$ -emulsion	$1.47 \pm .05$	$1.14 \pm .03$	$.476 \pm .012$	$2.40 \pm .11$
$^{28}\text{Si}$ -emulsion	$1.82 \pm .11$	$1.37 \pm .09$	$.422 \pm .015$	$2.60 \pm .14$

Table 5 represents the dispersion values of the multiplicity distribution for the singly charged, doubly charged, multi-charged projectile fragments and shower particles in  $^{16}\text{O}$ -emulsion,  $^{22}\text{Ne}$ -emulsion and  $^{28}\text{Si}$ -emulsion interactions at an incident momentum of (4.1-4.5) AGeV/c for the peripheral events (events without target fragmentation,  $N_h = 0$ ).

**Table 6**

Fragmentation Mode	<sup>16</sup> O- emulsion	<sup>22</sup> Ne- emulsion	<sup>28</sup> Si-emulsion
One Projectile Fragments with Z>2	51.81%	72.47%	76.60%
Two Projectile Fragments with Z>2	0%	1.12%	2.33%
Projectile Fragments with Z>2 and $\alpha$ particles	22.72%	41.94%	51.46%
Projectile Fragments with Z>2 and no $\alpha$ particles	29.09%	33.02%	28.07%

Table 6 represents the percentage of different fragmentation mode of multi-charged projectile fragments in peripheral collisions of <sup>16</sup>O-emulsion, <sup>22</sup>Ne-emulsion and <sup>28</sup>Si-emulsion interactions at an incident momentum of (4.1-4.5) AGeV/c.

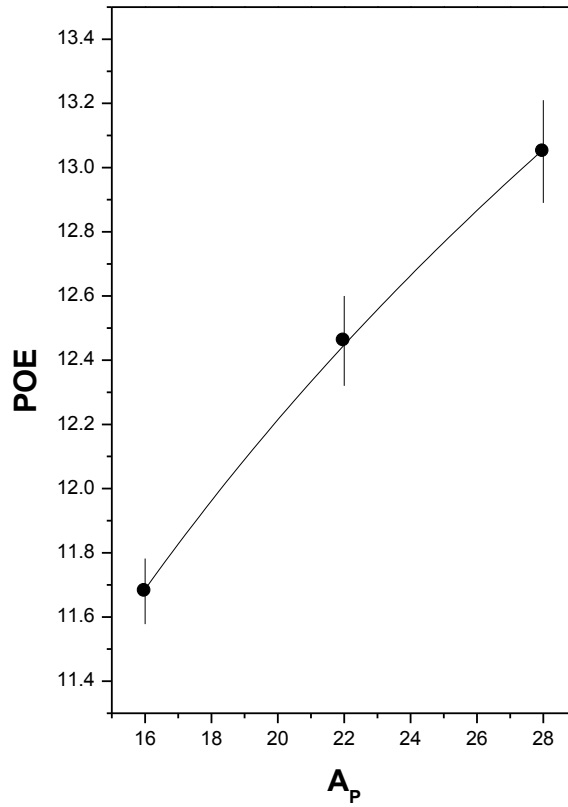


Fig1 Variation of the percentage of peripheral events (events without target fragmentation,  $N_h = 0$ ) with the mass number of the projectile beam for  $^{16}\text{O}$ -emulsion,  $^{22}\text{Ne}$ -emulsion and  $^{28}\text{Si}$ -emulsion interactions at an incident momentum of (4.1-4.5)AGeV/c. The solid line represents the non linear fit  $\text{POE} = aA_p^b$ .

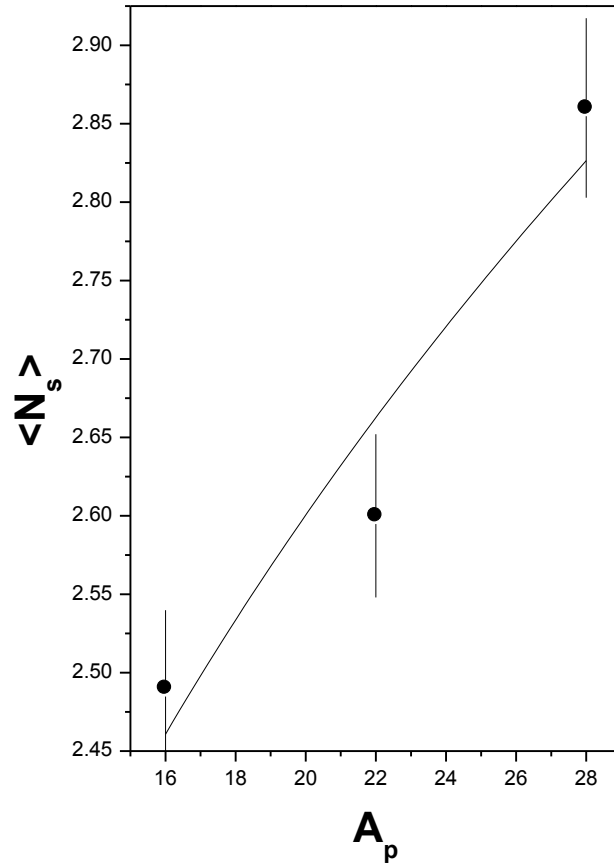


Figure 2 The variation of average multiplicity of shower particles with the mass number of the projectile beam for  $^{16}\text{O}$ -emulsion,  $^{22}\text{Ne}$ -emulsion and  $^{28}\text{Si}$ -emulsion interactions at an incident momentum of (4.1-4.5)A GeV/c for the peripheral events (events without target fragmentation,  $N_h = 0$ ). The solid line represents the non linear fit  $\langle N_s \rangle = aA_p^b$ .

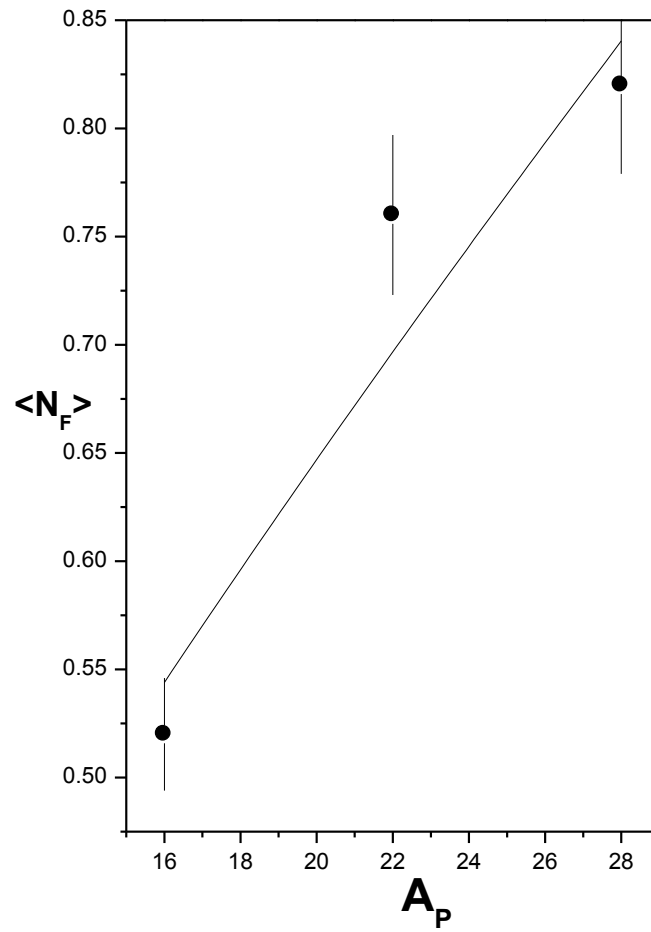


Figure 3 The variation of average multiplicity of multi-charged fragments ( $Z>2$ ) with the mass number of the projectile beam  $A_P$  for  $^{16}\text{O}$ -emulsion,  $^{22}\text{Ne}$ -emulsion and  $^{28}\text{Si}$ -emulsion interactions at an incident momentum of (4.1-4.5)AGeV/c for the peripheral events (events without target fragmentation,  $N_h = 0$ ). The solid line represents the non linear fit  $\langle N_F \rangle = aA_P^b$ .

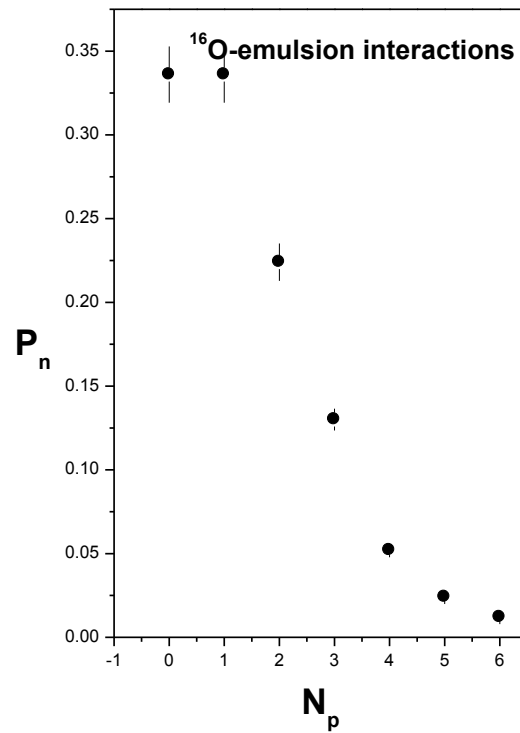


Figure 4(a) Multiplicity distribution of projectile fragments with  $Z=1$  for  $^{16}\text{O}$ -emulsion interactions at an incident momentum of 4.5 AGeV/c for the peripheral events (events without target fragmentation,  $N_h=0$ ).

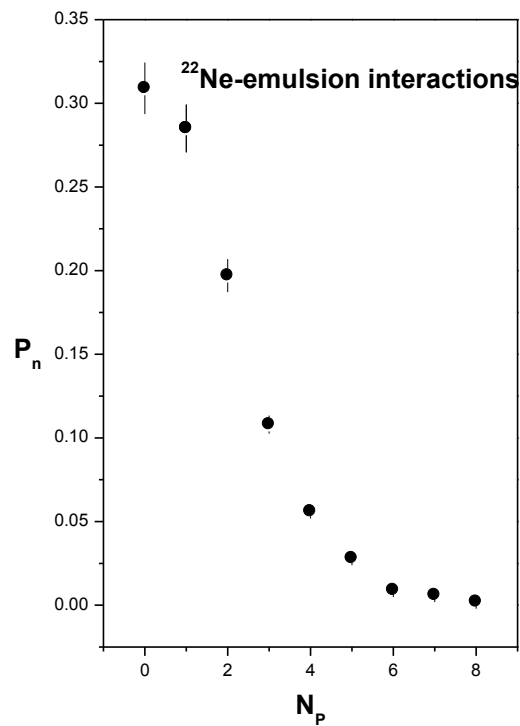


Figure 4(b) Multiplicity distribution of projectile fragments with  $Z=1$  for  $^{22}\text{Ne}$ -emulsion interactions at an incident momentum of 4.1 AGeV/c for the peripheral events (events without target fragmentation,  $N_h = 0$ ).

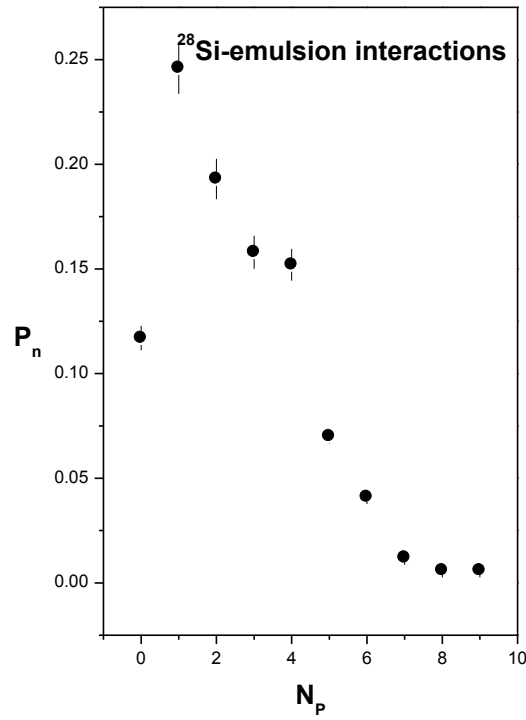


Figure 4(c) Multiplicity distribution of projectile fragments with  $Z=1$  for  $^{28}\text{Si}$ -emulsion interactions at an incident momentum of 4.5 AGeV/c for the peripheral events (events without target fragmentation,  $N_h = 0$ ).

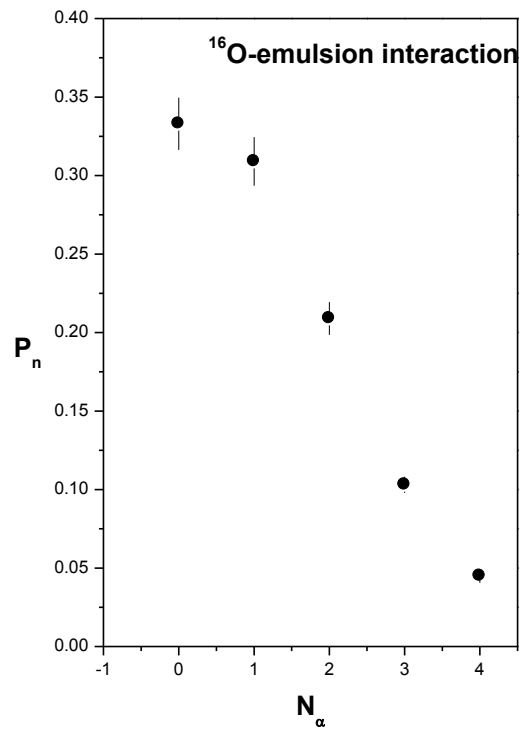


Figure 5(a) Multiplicity distribution of projectile fragments with  $Z=2$  for  $^{16}\text{O}$ -emulsion interactions at an incident momentum of 4.5 AGeV/c for the peripheral events (events without target fragmentation,  $N_h = 0$ ).

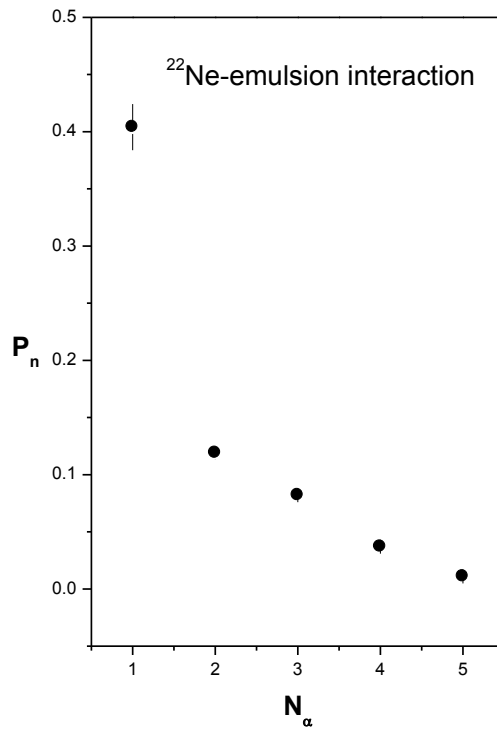


Figure 5(b) Multiplicity distribution of projectile fragments with  $Z=2$  for  $^{22}\text{Ne}$ -emulsion interactions at an incident momentum of 4.1 AGeV/c for the peripheral events (events without target fragmentation,  $N_h = 0$ ).

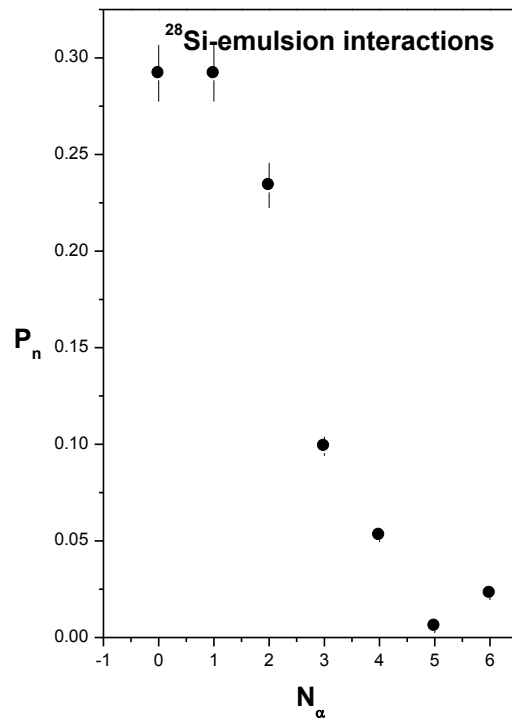


Figure 5(c) Multiplicity distribution of projectile fragments with  $Z=2$  for  $^{28}\text{Si}$ -emulsion interactions at an incident momentum of  $4.5 \text{ AGeV}/c$  for the peripheral events (events without target fragmentation,  $N_h=0$ ).

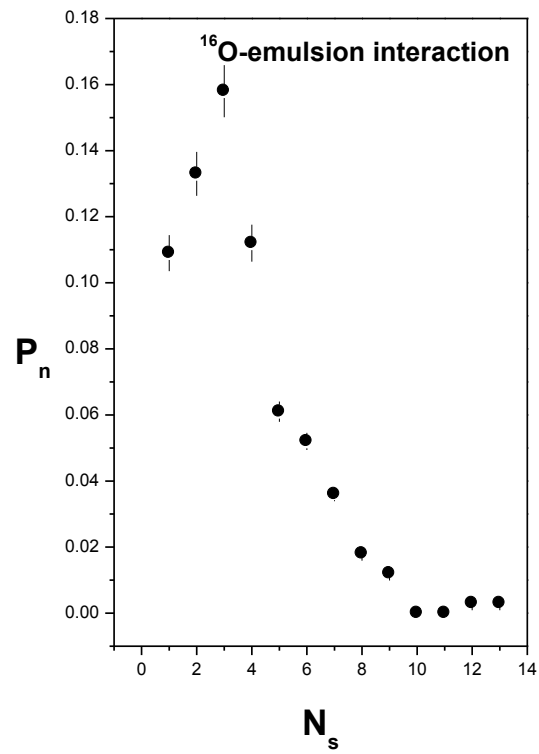


Figure 6(a) Multiplicity distribution of shower particles for  $^{16}\text{O}$ -emulsion interactions at an incident momentum of 4.5 AGeV/c for the peripheral events (events without target fragmentation,  $N_h = 0$ ).

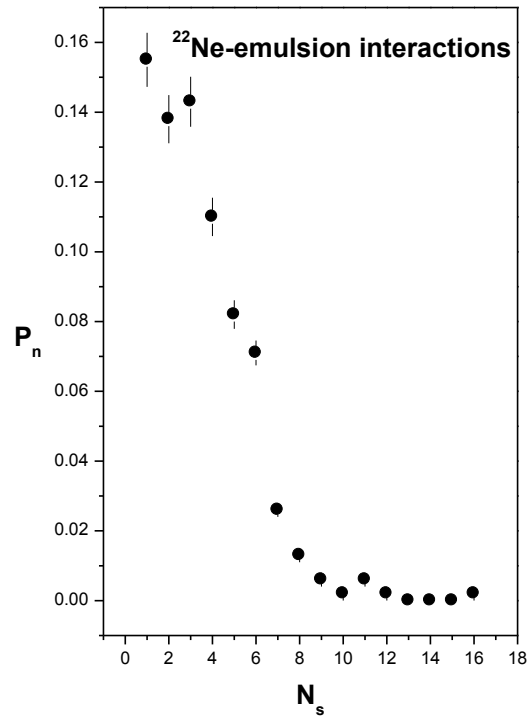


Figure 6(b) Multiplicity distribution of shower particles for  $^{22}\text{Ne}$ -emulsion interactions at an incident momentum of 4.1 AGeV/c for the peripheral events (events without target fragmentation,  $N_h = 0$ ).

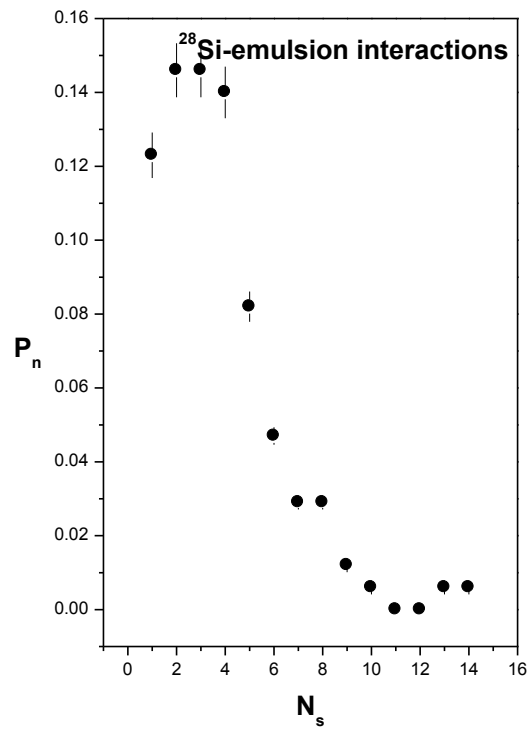


Figure 6(c) Multiplicity distribution of shower particles for <sup>28</sup>Si-emulsion interactions at an incident momentum of 4.5 AGeV/c for the peripheral events (events without target fragmentation, N<sub>h</sub> =0).

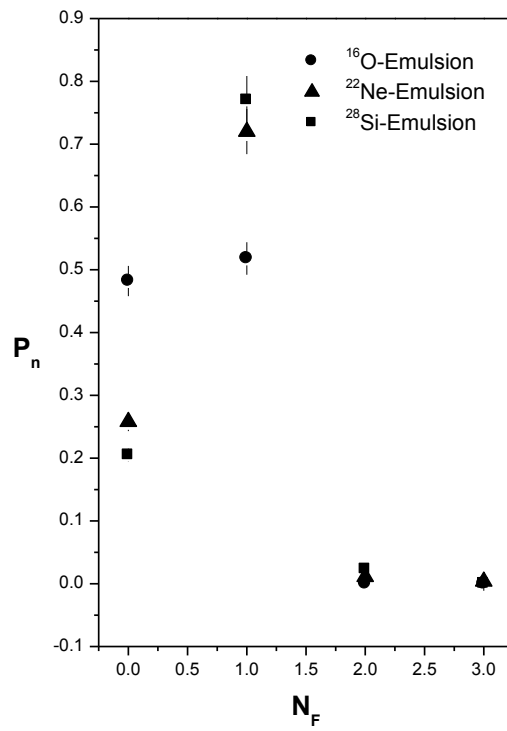


Figure 7 Multiplicity distribution of multi-charged projectile fragments of  $^{16}\text{O}$ -emulsion,  $^{22}\text{Ne}$ -emulsion and  $^{28}\text{Si}$ -emulsion interactions at an incident momentum of (4.1-4.5) AGeV/c for the peripheral events (events without target fragmentation,  $N_h = 0$ ).